



Effect of bonding temperature and heat treatment on microstructure and mechanical property of Mg–6Gd–3Y alloy vacuum diffusion bonded joints

Ping-yi MA^{1,2}, Xu CHEN^{1,2}, Xing HAN^{1,2}, Zhi-qiang LUO^{1,2}, He-li PENG^{1,2}

1. Shanghai Spaceflight Precision Machinery Institute, Shanghai 201600, China;

2. Shanghai Engineering Technology Research Center of Near-Net Shape Forming for Metallic Materials, Shanghai 201600, China

Received 29 June 2021; accepted 22 December 2021

Abstract: Diffusion bonding of as-cast Mg–6Gd–3Y magnesium alloy was carried out at temperatures of 400–480 °C with bonding pressure of 6 MPa for 90 min. Diffusion bonded joints were solution treated at 495 °C for 14 h and then aged at 200 °C for 30 h. Microstructures and mechanical properties of joints were analyzed. The results showed that rare earth elements and their compounds gathering at bonding interface hindered the grain boundary migration crossing bonding interface. Tensile strength of as-bonded and as-solution treated joints increased firstly and then decreased with the bonding temperature increasing due to the combined effects of grain coarsening and solid-solution strengthening. As-bonded and solution-treated joints fractured at matrix except the joint bonded at 400 °C, while aged joints fractured at bonding interface. The highest ultimate tensile strength of 279 MPa with elongation of 2.8% was found in joint bonded at 440 °C with solution treatment followed by aging treatment.

Key words: Mg–Gd–Y alloy; vacuum diffusion bonding; post-weld heat treatment; bonding interface; bonding strength

1 Introduction

Magnesium alloy containing rare earth elements (REs) is one of the important engineering structure materials used in many fields such as aerospace, automotive and 3C industries because of its low density, high specific strength and good castability [1–4]. There are many manufacturing methods for the forming of Mg alloy parts promoting the wide application of Mg alloy jointly, one of which is welding, including fusion welding, friction stir welding, brazing and vacuum diffusion bonding [5–10]. It is known that each welding method has its advantages and disadvantages when it is used to joint different materials and structures. For example, fusion welding has high efficiency in joining separated parts, but it may cause defects

of oxidative impurities, thermal cracks and deformation due to the properties of low melting point, high linear expansion coefficient and large thermal conductivity of Mg alloys. It is challenging for fusion welding and friction stir welding methods to joint components with complicated internal structures. Corrosion problem will be introduced when brazing due to the addition of filler metal. Vacuum diffusion bonding is a solid-state joining method and there are no fusion welding defects and heat affected zone in the bonded joint. In addition, diffusion bonded joint obtained under optimized process parameters is always with high strength and dimensional accuracy. Consequently, diffusion bonding has special advantages especially for the precision joining of Mg alloy parts with complicated internal structures, such as waveguide component, vapor chamber and hollow aircraft rudder.

Most study of diffusion bonding about Mg alloys focused on Mg–Al or Mg–Zn series wrought Mg alloys [9,10], but that about Mg alloys strengthened by REs was just a little. TONG et al [11] studied the evolution of microstructure and mechanical properties of as-cast Mg–8Gd alloy diffusion bonded joints at various bonding temperatures. It was reported that the tensile strength of joints increased firstly and then decreased with the increase of bonding temperature from 500 to 560 °C, and the joint formed at 550 °C exhibited the highest tensile strength of 151 MPa. Thus, temperature has great effect on mechanical performance of diffusion bonded joint. But grains of the α -Mg matrix coarsened greatly because of the high bonding temperature resulting strength of the joint was barely satisfactory. It has been reported that heat treatment is one of the effective methods for improving mechanical performance of Mg–REs alloys [12–14]. Mg–REs alloys are equivalent to be solution treated incompletely during diffusion bonding process, so the alloys may need to be solution treated thoroughly and aging treated to gain a good mechanical performance after diffusion bonding process. However, no study about the effect of post-weld heat treatment on diffusion bonded joints of Mg–REs alloys has been performed so far. Mg–Gd–Y series alloys are representative among Mg–REs alloys, one of which Mg–6Gd–3Y alloy has a good combination of strength and ductility [12]. So that the main purpose of this study is to research the effect of bonding temperature and post-weld heat treatment on microstructure and mechanical properties of Mg–6Gd–3Y alloy diffusion bonded joints.

2 Experimental

The base material employed in this work was a Mg–6Gd–3Y (below denoted by GW63) cast ingot with actual composition of Mg–5.83Gd–2.91Y–0.46Zr (mass fraction, %). The material was prepared from high-purity Mg (>99.95 wt.%), Mg–25Gd (wt.%), Mg–25Y (wt.%) and Mg–30Zr (wt.%) master alloys in an electric resistance furnace under the mixed atmosphere of CO₂ and SF₆ with a volume ratio of 100:1. Then, the melt was poured into sand mold. The ingot was machined into block specimens (50 mm × 40 mm × 35 mm) and the surfaces to be bonded were with the size of 50 mm in length and 35 mm in width. Prior to bonding, the mating surfaces were polished by conventional grinding techniques with final grinding on 1500 grit sandpaper to remove the oxide film. The specimens were ultrasonically cleaned and dried in air, and then assembled as shown in Fig. 1(a).

Bonding parameters, such as temperature, pressure and holding time affect joint performance greatly. Typical diffusion bonding temperature for metal is $0.7T_m$ (T_m , melting point of the metal to be bonded) [15]. According to the phase diagram of Mg–xGd–3Y [16], liquidus temperature of GW63 alloy is about 600 °C, so it can be speculated that the typical bonding temperature for GW63 alloy is around 420 °C. And temperature of REs totally dissolving into matrix is about 455 °C, when grain boundary of α -Mg grain will migrate more easily. So the bonding temperatures were chosen as 400, 420, 440, 460 and 480 °C, respectively. Plastic

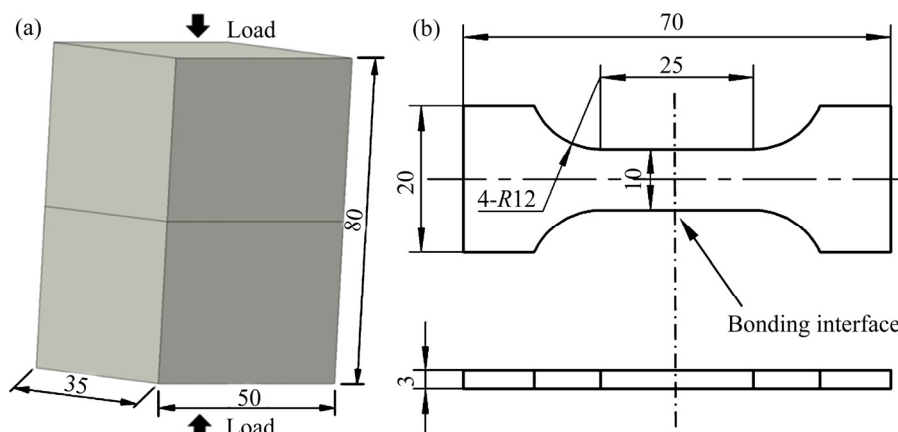


Fig. 1 Schematics of diffusion bonded specimen assembling method (a) and size of tensile specimen (b) (unit: mm)

deformation of joint is mainly caused by the creep, which promotes the formation of sound joint. The high temperature creep mechanism is closely related to the stress level, and creep behavior is mainly through grain boundary creep when the stress varies from $0.2\sigma_s$ to $0.4\sigma_s$ (σ_s , yield strength at deformation temperature), while it is in agreement with plastic mechanism when stress is higher than $0.4\sigma_s$ [17]. So as to guarantee the bonding strength and avoid large deformation, bonding pressure was set at $0.2\sigma_s$. Yield strength of GW63 alloy is about 32 MPa at 450 °C with the strain rate of 0.001 s^{-1} [18], so the bonding pressure was set as 6 MPa. And bonding time was kept at 90 min.

During the bonding process, heating control program was started when the vacuum pressure was less than 5×10^{-3} Pa and heating rate was kept at 10 °C/min. A unique feature of magnesium is its high evaporation rate as compared to other metals [19], which is detrimental during vacuum diffusion bonding, causing rough surface of specimen and polluting furnace chamber. To prevent evaporation of Mg, the vacuum pump system was turned off and then the furnace chamber was refilled with high purity argon (99.99 wt.%) till the vacuum pressure reached 200–250 Pa when the temperature rose to 200 °C. The assemblies were cooled to room temperature in the processing furnace chamber after diffusion bonding.

Following diffusion bonding, three tensile test specimens with dimensions shown in Fig. 1(b) and one metallographic specimen were cut from each bonded specimen by wire cut electric discharge machine. Then, the rests of bonded specimens were heat treated in an electric furnace under the protection of SO_2 atmosphere and cooled in air, and heat treatment processes of T4 (solution treatment at 495 °C for 14 h) and T6 (aging treatment at 200 °C for 30 h following T4 treatment) for GW63 alloy were commonly used in the industrial production [12,13]. After T4 treatment, each bonded specimen was cut into three tensile test specimens and one metallographic specimen again. Finally, the final remained specimens were aged at 200 °C for 30 h and sampled for the third time.

Microstructures of joints with different heat treatments were observed by using GD60–DS optical microscope (OM) and FEI Nova 450 field emission gun scanning electron microscope (SEM). The samples for OM and SEM observations were

mechanically polished and then etched in an acetic acid glycol solution. The compositions of matrix and precipitations were characterized by using an energy dispersive X-ray spectrometer (EDS) equipped with the SEM. The grain sizes of samples were evaluated on the OM images using Image-Pro Plus software. Tensile tests were performed on CMT 5305 tensile test machine at a tensile speed of 1 mm/min. Fracture morphologies of tensile test specimens were examined by SEM.

3 Results and discussion

3.1 Macroscopic deformation characteristics

Deformation is inevitable to promote contact between mating surfaces and obtain the diffusion bonded joint with satisfying mechanical performance. However, larger deformation may lead to the failure of parts. In this work, deformation ratio was used to characterize the macroscopic deformation of diffusion bonded joint, which referred to the ratio of the height change before and after bonding process to the height before bonding process. Deformation ratios at different bonding temperatures are illustrated in Fig. 2. It shows that deformation ratio increases with the increase of bonding temperature. As the bonding temperature increased from 400 to 480 °C, the deformation ratio increased from 0.14% to 3.7%. And the deformation ratio did not exceed 1% when bonding temperature was lower than 440 °C, while it was increased obviously when bonding temperature was higher than 440 °C. The regularity of deformation ratio change corresponds to the common sense that creep deformation of material is positively correlated to temperature under constant stress and time.

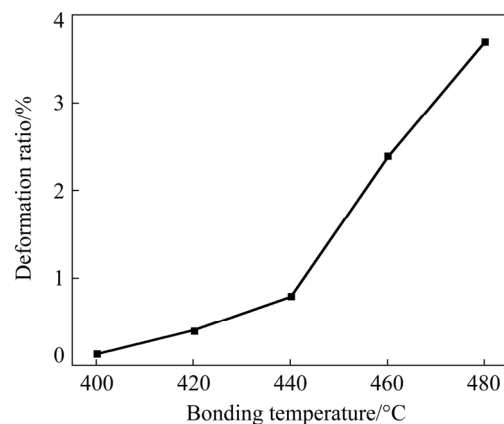


Fig. 2 Deformation ratios of GW63 joints bonded under pressure of 6 MPa for 90 min at different temperatures

3.2 Microstructure

The microstructure of the as-cast GW63 base metal prepared for diffusion bonding is shown in Fig. 3. The base metal was mainly formed by the equiaxial α -Mg matrix and eutectic phase mixed with $Mg_{24}Y_5$ and Mg_5Gd along the grain boundaries [20]. The black spots dispersed in α -Mg matrix were rich in Zr element which was used as nucleating agent to refine grains in the solidification process of cast alloy. The mean size of α -Mg grains was about $67\ \mu\text{m}$ which was measured by linear intercept method. Figure 4 shows the microstructures of GW63 alloy joints diffusion bonded at various temperatures. The dark bond lines in optical morphologies of all joints indicated the location of bonding interface. And all of these joints were bonded well since there were no obvious pores at the bonding interfaces. Curve of mean grain sizes of joints at different diffusion bonding temperatures is shown in Fig. 5. It shows that α -Mg grains grow up slightly with bonding temperature increasing from 400 to 480 °C.

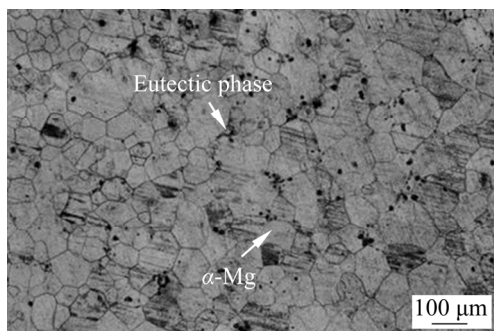


Fig. 3 Optical morphology of as-cast GW63 alloy

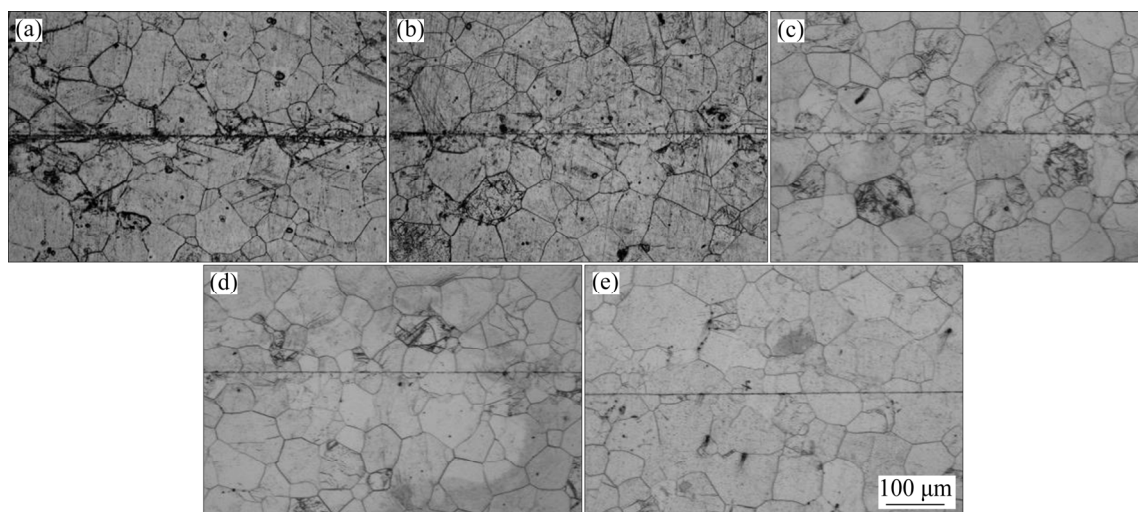


Fig. 4 Optical morphologies of GW63 alloy joints diffusion bonded at various temperatures: (a) 400 °C; (b) 420 °C; (c) 440 °C; (d) 460 °C; (e) 480 °C

Therefore, phenomenon of grain boundary migration happened during diffusion bonding process. However, there were almost no grains across the bonding interface in all of these joints.

Figure 6 shows the SEM images of joints bonded at 400, 440 and 480 °C and corresponding EDS maps. As shown in Fig. 6, the bond lines were decorated by some bright phases and the number of bright phases increased with bonding temperature increasing. According to EDS maps, there were more Y, Gd and O elements at bonding interfaces of joints bonded at 440 and 480 °C than base metals, while joint bonded at 400 °C was with more uniform distributions of these elements along the direction perpendicular to bonding interface. EDS results of points in Fig. 6 are listed in Table 1. It can be seen that both the contents of Gd and Y in bright phase were higher than those in base metal. And the content of Y was higher than that of Gd in bright phase when bonding temperature was higher than 400 °C, while this comparison was contrary in base metal.

At the beginning of diffusion bonding process, there were large amount of micro voids between the mating surfaces and these micro voids closed during bonding process. The process of void closing can be accelerated by deformation of asperities between the mating surfaces, atomic diffusion and formation of new phase [21,22]. Since there are many defects such as micro voids at bonding interface, RE atoms will diffuse and gather at bonding interface spontaneously to reduce interface energy and form compounds with Mg and O

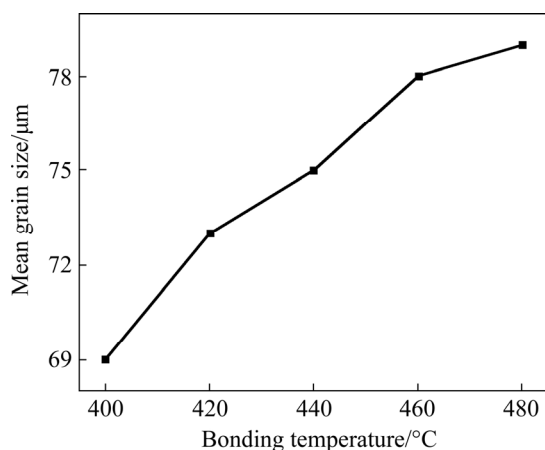


Fig. 5 Mean grain sizes of joints diffusion bonded at different temperatures

atoms [11]. As a result, RE atoms and their compounds accelerated the closure of interfacial voids, and bright phases at the bonding interface might indicate the existence of micro voids which were full filled by new phases during bonding process.

REs present good affinity to oxygen when compared with Mg and the affinity to oxygen of Y is larger than that of Gd [19]. As the ratio of molar fraction of O over that of REs is close to 1.5 according to EDS results shown in Table 1, the main form of O element presented at the bonding interface might be RE_2O_3 . According to the Mg-xGd-3Y phase diagram [16], when Mg-6Gd-3Y alloy was heated up continuously, the precipitated phase of Mg_{24}Y_5 was first to be dissolved into α -Mg matrix at about 280 °C, while Mg_5Gd phase was dissolved at about 455 °C. Thus, the number of Y atoms which could diffuse freely was more than that of Gd atoms during the heating process of diffusion bonding. Diffusion coefficients of Y and Gd in hcp Mg are similar to each other and almost one order of magnitude lower than self-diffusion coefficient Mg [23]. It is known that diffusion coefficient is greatly affected by temperature and increases with the increase of temperature. As a result, there was no obvious phenomenon that REs gathered at the bonding

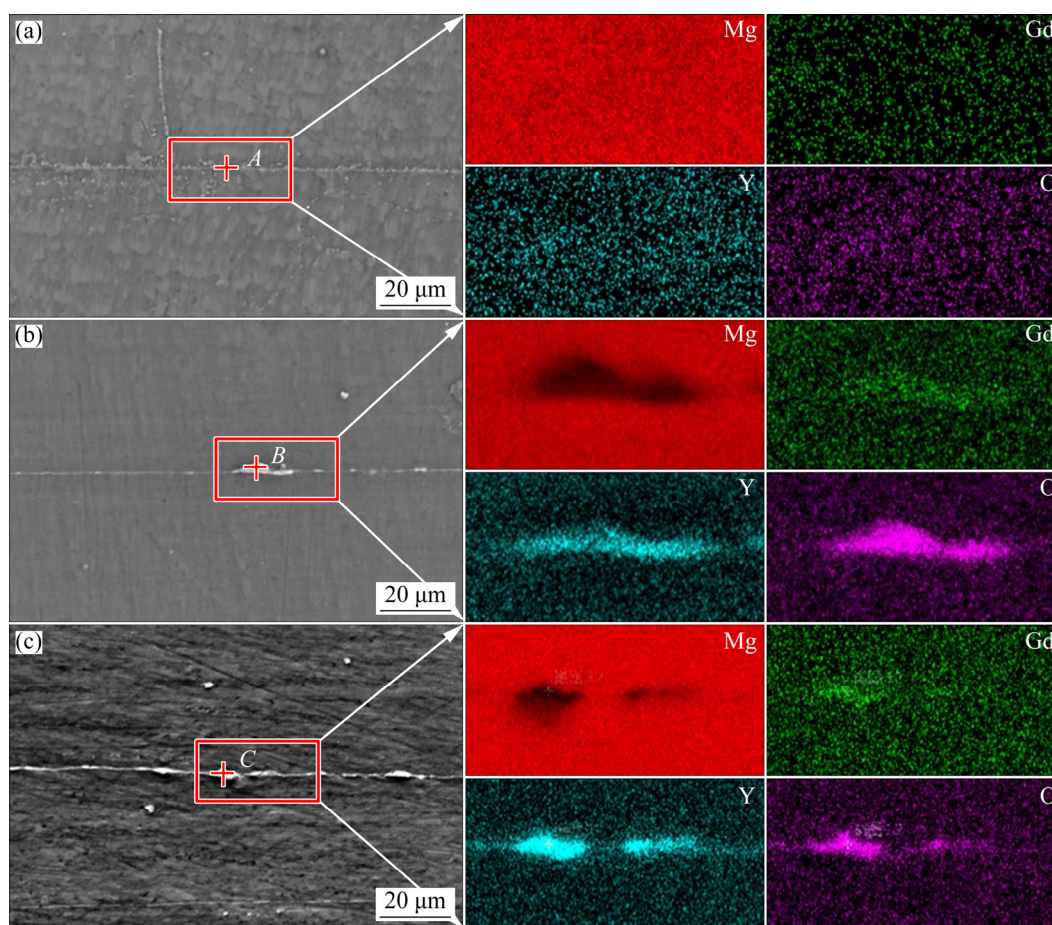


Fig. 6 SEM images and corresponding EDS maps of GW63 joints diffusion bonded at various temperatures: (a) 400 °C; (b) 440 °C; (c) 480 °C

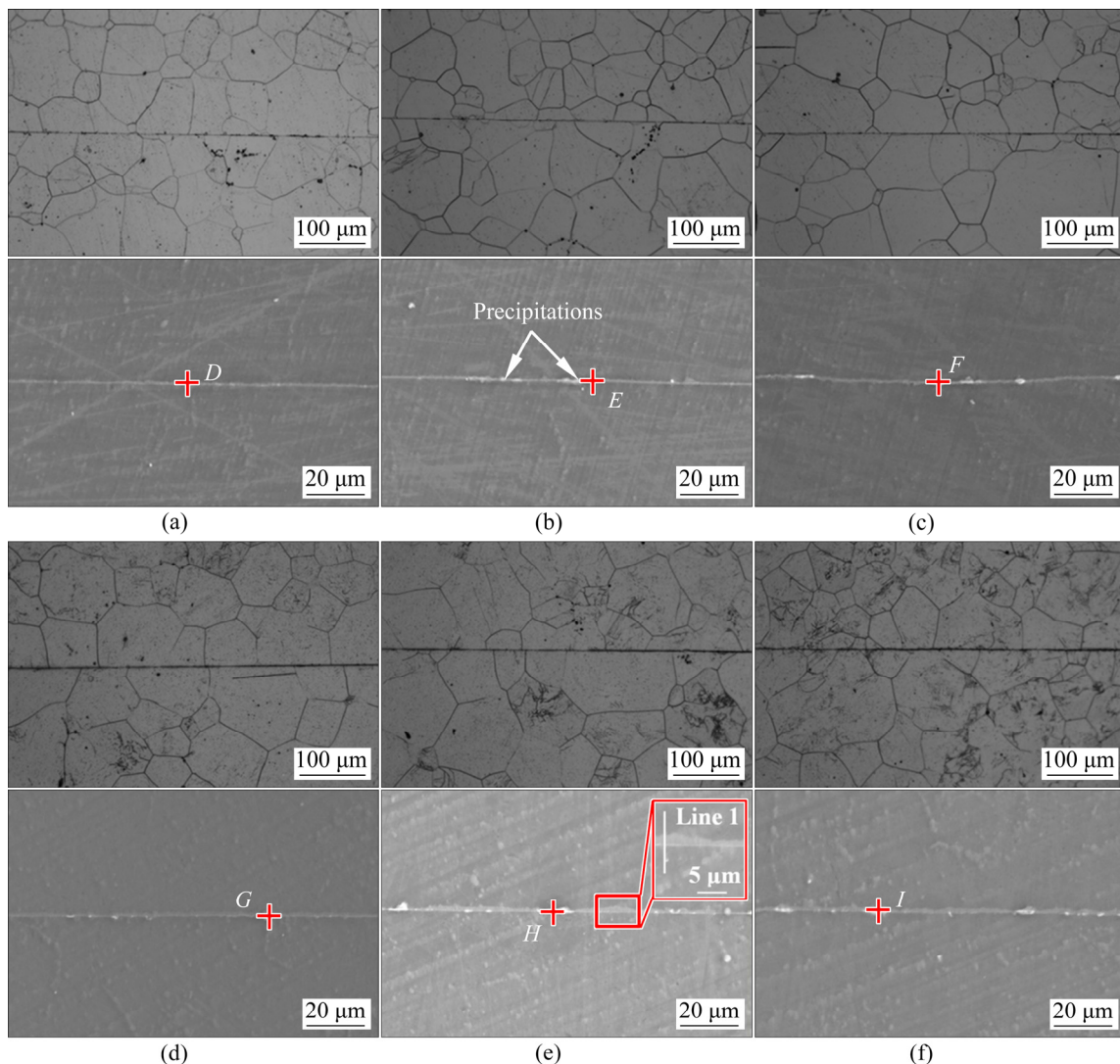
Table 1 EDS results of different points shown in Fig. 6 (at.%)

Point No.	Mg	Gd	Y	O
<i>A</i>	94.95	1.4	0.97	2.68
<i>B</i>	91.38	1.85	2.35	4.42
<i>C</i>	70.96	2.31	8.68	18.05

interface when joint was bonded at 400 °C due to the lower diffusion coefficients of Gd and Y according to the composition of Point *A* shown in Table 1. While the sum of molar fractions of Gd and Y in bright phases at bonding interface increased to 10.99% as bonding temperature increased to 480 °C, and there were more Y atoms at the bonding interface than Gd atoms when temperature was higher than 400 °C. The effect of REs on grain refinement to magnesium alloy is attributed to the

hindering of REs distributing along the grain boundary to grain coarsening [24]. So that REs and their compounds distributing at the bonding interface hindered the grain boundary migration crossing the bonding interface, resulting that there were almost no grains across bonding interface during the bonding process.

Figure 7 shows the microstructures of heat treated joints bonded at 400, 440 and 480 °C. It can be found that most of precipitations in the base metal were dissolved into α -Mg matrix after T4 treatment at 495 °C for 14 h, while the bright phases still existed at bonding interfaces according to SEM images. So the phenomenon of REs enrichment at bonding interface was hard to be eliminated after solution treatment since oxides of REs were hard to decompose during T4 treatment. The mean grain sizes of joints bonded at different

**Fig. 7** Optical and corresponding SEM micrographs of T4-treated joints bonded at 400 °C (a), 440 °C (b) and 480 °C (c), and T6-treated joints bonded at 400 °C (d), 440 °C (e) and 480 °C (f)

temperatures after T4 treatment are shown in Fig. 8. It can be seen that α -Mg grains of all joints grew up slightly compared to the grains of as-bonded joints due to the dissolution of Mg_5Gd and $Mg_{24}Y_5$ phases. In addition, joints bonded at different temperatures experienced different thermal cycles, and joint bonded at higher temperature was equivalent to be solution treated for longer time during the same T4 treatment. So as shown in Fig. 8, mean grain size of T4-treated joint increased with the increase of the original bonding temperature. According to Figs. 7(d–f), the optical microstructures of T6 treated joints were similar to those of T4-treated ones, and the grain size almost did not change during aging treatment. As same as the T4-treated joints, there were precipitations at the bonding interfaces of T6-treated joints yet.

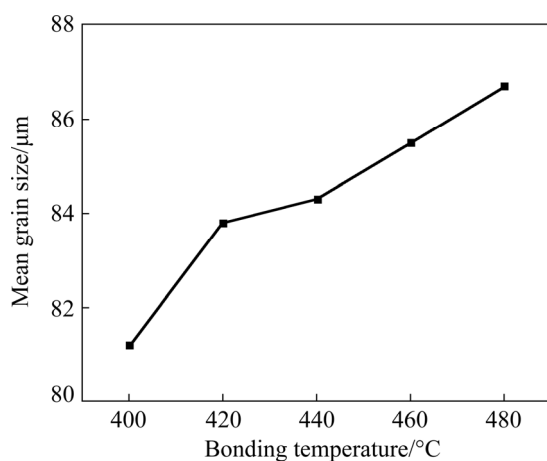


Fig. 8 Mean grain sizes of T4-treated joints bonded at different temperatures

Compositions of precipitations at bonding interfaces of joints bonded at different temperatures and with different heat treatments are shown in Table 2. It can be found that the content of Gd decreased, while content of Y increased slightly when joints underwent T4 treatment. It might be because Y atoms continued to diffuse to the bonding interface and Gd atoms in Gd_2O_3 were substituted by Y atoms during T4 treatment due to the larger affinity to oxygen of Y than that of Gd. However, the sum of molar fractions of Gd and Y increased after T4 treatment and even further after T6 treatment. According to the magnified SEM micrograph of zone in red rectangle shown in Fig. 7(e), there was a thin diffusion layer at bonding interface, and distributions of elements along Line 1 perpendicular to bonding interface are shown in

Fig. 9. It shows that there was a valley in the distribution curve of Mg and peaks of Y and O, and this phenomenon corresponded to EDS results shown in Table 2, and the thickness of diffusion layer was about 2 μm .

Table 2 EDS results of points shown in Fig. 7 (at.%)

Treatment	Point No.	Mg	Gd	Y	O
T4	D	94.05	1.01	1.32	3.62
	E	89.82	0.89	3.96	5.33
	F	65.86	1.93	10.9	21.31
T6	G	93.54	1.09	1.53	3.84
	H	89.39	1.35	4.10	5.16
	I	62.62	1.81	11.77	23.80

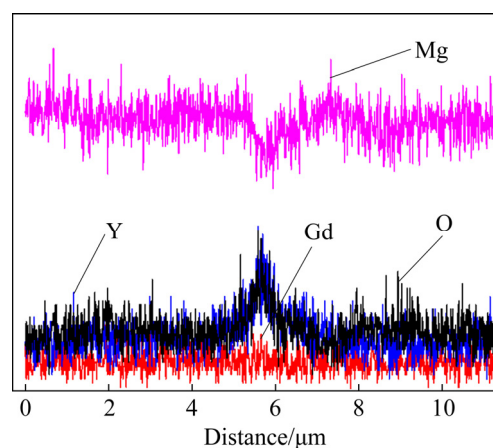


Fig. 9 Distribution of elements along Line 1 shown in Fig. 7(e)

3.3 Mechanical properties

Tensile test results of GW63 joints diffusion bonded at different temperatures and heat treated under different conditions are illustrated in Fig. 10. As shown in Fig. 10(a), tensile strength of as-bonded joint was equivalent to that of as-cast base metal with tensile strength of 208 MPa. When bonding temperature increased from 400 to 480 $^{\circ}C$, tensile strength of joints increased firstly and then decreased a little, and joint bonded at 440 $^{\circ}C$ had a peak tensile strength of 211 MPa. Meanwhile, elongation increased from 1.6% to 5.4% as shown in Fig. 10(b). After T4 treatment, both tensile strength and elongation of joints increased firstly and then decreased with original bonding temperature increasing. Joint bonded at 440 $^{\circ}C$ had yet the peak tensile strength of 220 MPa with an elongation of 8.2%. After T6 treatment, tensile

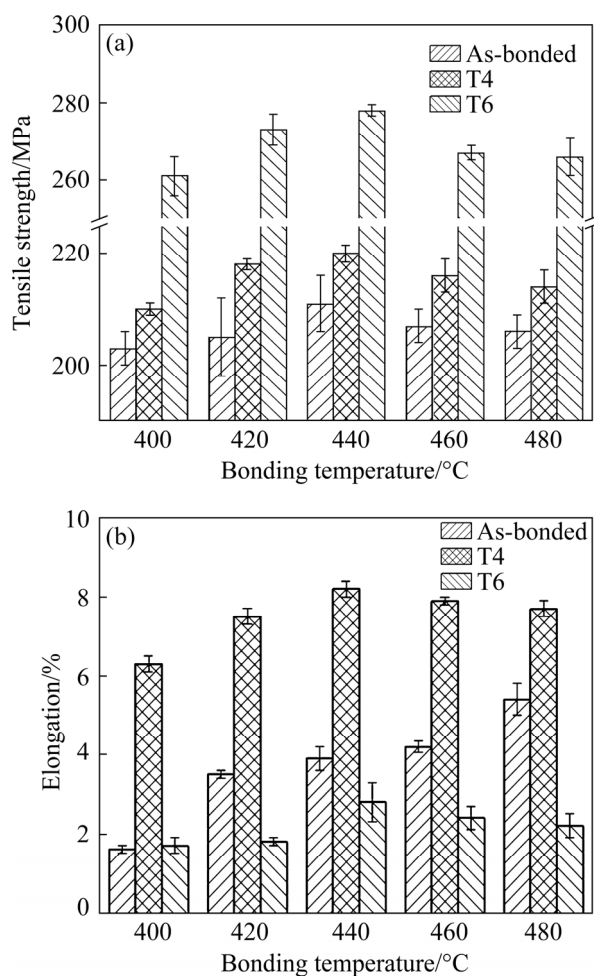


Fig. 10 Mechanical properties of joints bonded at different temperatures with different heat treatments: (a) Tensile strength; (b) Elongation

strength and elongation of joints showed the same trend as those of T4-treated joints. And tensile strength of joint bonded at 440 °C reached the maximum of 279 MPa, equivalent to 91% that of T6-treated base metal, while its elongation was mere 3.5%. So tensile strength of joint was improved slightly after T4 treatment while significantly after T6 treatment, and ductility decreased greatly after T6 treatment.

After tensile test, all joints as-bonded and T4-treated fractured at base metal except joint bonded at 400 °C fracturing at bonding interface, and all T6-treated joints fractured at bonding interface. Fracture morphologies of tensile test specimens are shown in Fig. 11. According to Figs. 11(a–c), fracture surface of joint bonded at 400 °C was smooth and there were scratches on the fracture surface. These scratches were introduced during polish process before bonding and did not disappear

during bonding process. Figure 11(b) shows that there were some areas fracturing at base metal during tensile test of T4-treated joint bonded at 400 °C, so the elongation increased compared to as-bonded state. According to Figs. 11(d–g), fracture morphologies of joints bonded at 440 °C with different heat treatments and T6-treated base metal were composed of cleavage planes and many tear ridges, which indicated that the fracture mode was transgranular quasi-cleavage fracture; and smooth fracture morphologies of T6-treated joints indicated the brittle fracture mode. In addition, there were some precipitates linearly distributing on the fracture surface shown in Fig. 11(f). It may be contributed to the scratch, along which micro tunnel hole formed at the initial contact of mating surfaces; and the tunnel holes were fully filled by precipitates and deformed base metal. EDS maps of rectangular region in Fig. 11(f) show that the precipitate was rich in Y and O elements; its composition shown in Fig. 11(i) virtually corresponded to the results shown in Table 2, while the few Gd and Y might be because there were traces of α -Mg matrix on the surface of precipitate.

According to the tensile test results and microstructure analysis, sample was equivalent to being solution treated for a short time during bonding process. It is known that grain coarsening and solid-solution strengthening can occur during T4 treatment. Grain coarsening is mainly determined by diffusion of Mg and solid-solution strengthening is mainly determined by diffusion of REs. Meanwhile, grain coarsening has negative effect while solid-solution strengthening has positive effect on tensile strength of metal. So, the final tensile strength of metal is affected by the combined effects of grain coarsening and solid-solution strengthening. Both grain coarsening and solid-solution strengthening are affected by temperature greatly. When bonding temperature was not higher than 440 °C, precipitates were dissolved incompletely and grains grew up slightly. At meantime, solid-solution strengthening effect of REs was not outstanding due to the less amount and lower diffusion coefficients of free RE atoms. Tensile strength of bonding interface of joint bonded at 400 °C was lower than that of base metal since there were few REs diffusing to the bonding interface inducing insufficient strengthening effect on the bonding interface. Tensile strength of joint

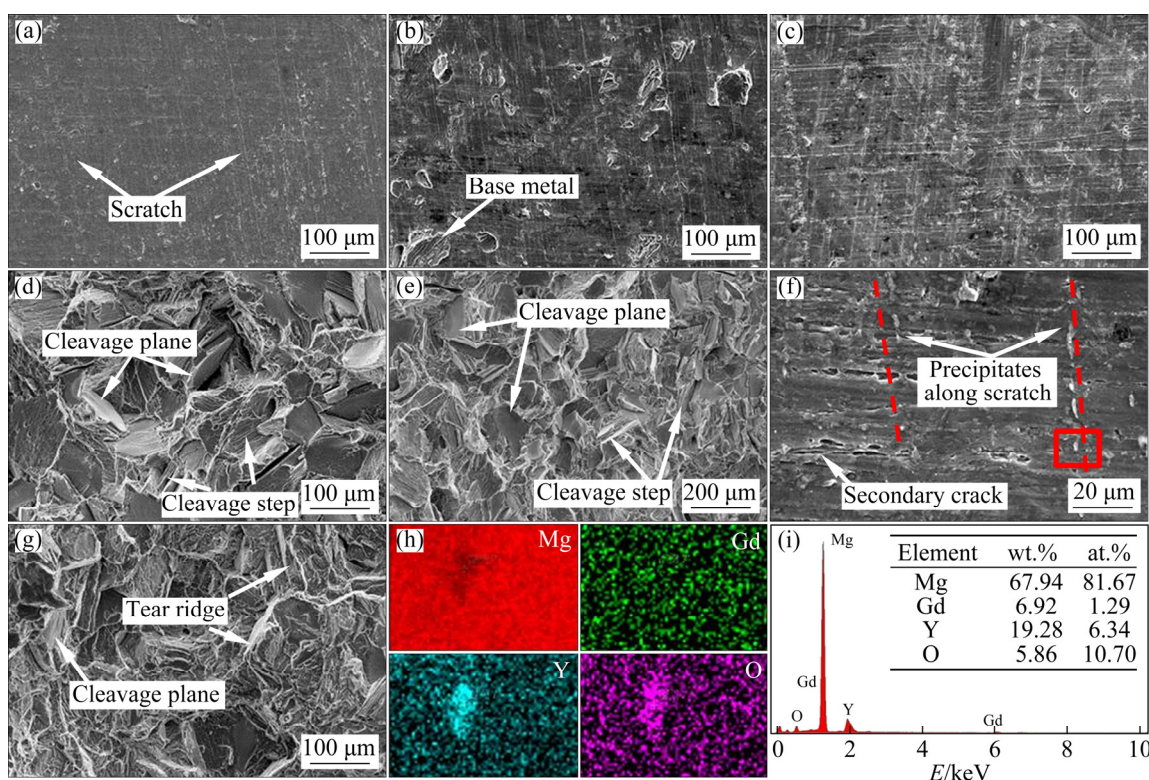


Fig. 11 Tensile fracture morphologies of joints bonded at 400 °C (a, b, c) and 440 °C (d, e, f): (a, d) As-bonded; (b, e) T4-treated; (c, f) T6-treated; (g) T6-treated base metal; EDS maps (h) and composition of precipitate (i) in rectangular region of (f)

bonded at 420 °C was slightly lower than that of as-cast base metal due to the partly dissolving of precipitate. And tensile strength of joint bonded at 440 °C was slightly high due to the effect of solid-solution strengthening of REs. When bonding temperature was higher than 440 °C, grain coarsening had greater effect on mechanical property of base metal than solid-solution strengthening due to the larger diffusion coefficient of Mg than that of REs. Thus, the tensile strength of base metal decreased slightly with bonding temperature increasing from 440 to 480 °C.

After T4 treatment, REs had diffused enough, enhancing the effect of solid-solution strengthening, so tensile strength of T4-treated joints is somewhat higher than that of bonded joints. With bonding temperature increasing, tensile strength of T4-treated joints increased firstly due to solid-solution strengthening and then decreased due to grain coarsening. After T6 treatment, both base metal and bonding interface were strengthened by precipitations, and there were more precipitates at the bonding interface than base metal owing to the higher content of REs at the bonding interface. With

the increase of bonding temperature, the amount of REs contained at the bonding interface increased, promoting the effect of precipitation strengthening on bonding interface and resulting in the increase of brittleness at the meantime. As a result, all of these joints fractured at bonding interface since cracks could originate and propagate easily around precipitates, leading to the lower strength and ductility than base metal. Tensile strength and elongation of T6-treated joints decreased to some extent when the bonding temperatures were higher than 440 °C since there were too many precipitates at the bonding interface.

4 Conclusions

(1) The deformation ratio increased with increase in bonding temperature, which did not exceed 1% at the bonding pressure of 6 MPa for 90 min when bonding temperature was lower than 440 °C while it increased obviously when bonding temperature was higher than 440 °C.

(2) REs diffusion to the bonding interface hindered the grain boundary migration crossing the

bonding interface during bonding process. With bonding temperature increasing, the amount of REs contained at bonding interface and grain size of joints increased. Grains of as-bonded joints coarsened slightly after T4 treatment and almost did not change during aging process.

(3) Tensile strength of as-bonded joints and heat-treated joints increased firstly and then decreased with the bonding temperature increasing due to the combined effects of grain coarsening and solid-solution strengthening. As-bonded and T4-treated joints fractured at matrix except joint bonded at 400 °C, while T6-treated joints fractured at bonding interface. Better mechanical properties with tensile strength of 279 MPa and elongation of 2.8% were found in joint bonded at 440 °C and solution treated at 495 °C for 14 h followed by aging treatment at 200 °C for 30 h.

Acknowledgment

This work was financially supported by the Science Innovation Foundation of Shanghai Academy of Spaceflight Technology, China (No. SAST2020-117).

References

- [1] MU Y L, WANG Q D, HU M L, JANIK V, YIN D D. Elevated-temperature impact toughness of Mg-(Gd,Y)-Zr alloy [J]. *Scripta Materialia*, 2013, 68: 885–888.
- [2] JIA Lin-yue, DU Wen-bo, WANG Zhao-hui, LIU Ke, LI Shu-bo, YU Zi-jian. Dual phases strengthening behavior of Mg-10Gd-1Er-1Zn-0.6Zr alloy [J]. *Transactions of Nonferrous Metals Society of China*, 2020, 30: 635–646.
- [3] WANG Feng-hua, DONG Jie, FENG Miao-lin, SUN Jie, DING Wen-jiang, JIANG Yan-yao. A study of fatigue damage development in extruded Mg-Gd-Y magnesium alloy [J]. *Materials Science and Engineering A*, 2014, 589: 209–216.
- [4] DING Zhi-bing, ZHAO Yu-hong, LU Ruo-peng, YUAN Mei-ni, WANG Zhi-jun, LI Hui-jun, HOU Hua. Effect of Zn addition on microstructure and mechanical properties of cast Mg-Gd-Y-Zr alloys [J]. *Transactions of Nonferrous Metals Society of China*, 2019, 29: 722–734.
- [5] SHE Qing-yuan, YAN Hong-ge, CHEN Ji-hua, SU Bin, YU Zhao-hui, CHEN Chao, XIA Wei-jun. Microstructure characteristics and liquation behavior of fiber laser welded joints of Mg-5Zn-1Mn-0.6Sn alloy sheets [J]. *Transactions of Nonferrous Metals Society of China*, 2017, 27: 812–819.
- [6] SHARAH I H J, POURANVARI M, MOVAHEDI M. Enhanced resistance to liquation cracking during fusion welding of cast magnesium alloys: Microstructure tailoring via friction stir processing pre-weld treatment [J]. *Materials Science and Engineering A*, 2020, 798: 140142.
- [7] COMMINS L, DUMONT M, MASSE J E, BARRALLIER L. Friction stir welding of AZ31 magnesium alloy rolled sheets: Influence of processing parameters [J]. *Acta Materialia*, 2009, 57(2): 326–334.
- [8] YANG Tuo-yu, ZHANG Yang-yang, WANG Ke-hong, ZHANG De-ku, CHEN Feng, GUO Chun. Interface behaviour of brazing seam of contact-reaction brazing an AZ31 magnesium with amorphous filler metal [J]. *Journal of Manufacturing Processes*, 2021, 68: 683–689.
- [9] YU Yan-dong, LI Qiang. Diffusion bonding in superplastic ZK60 magnesium alloy [J]. *Materials Science Forum*, 2005, 488/489: 227–230.
- [10] SOMEKAWA H, HIGASHI K. Diffusion bonding in commercial superplastic AZ31 magnesium alloy sheets [J]. *Key Engineering Materials*, 2003, 233/234/235/236: 857–862.
- [11] TONG Xin, ZAI Le, YOU Guo-qiang, WU Hong, WEN Heng-yu, LONG Si-yuan. Effects of bonding temperature on microstructure and mechanical properties of diffusion-bonded joints of as-cast Mg-Gd alloy [J]. *Materials Science and Engineering*, 2019, 767: 138408.1–138408.13.
- [12] WANG Quan, XIAO Lv, LIU Wen-cai, ZHANG Hao-hao, CUI Wen-dong, LI Zhong-quan, WU Guo-hua. Effect of heat treatment on tensile properties, impact toughness and plane-strain fracture toughness of sand-cast Mg-6Gd-3Y-0.5Zr magnesium alloy [J]. *Materials Science and Engineering A*, 2017, 705: 402–410.
- [13] LI Sheng-yong, LI De-jiang, ZENG Xiao-qin, DING Wen-jiang. Microstructure and mechanical properties of Mg-6Gd-3Y-0.5Zr alloy processed by high-vacuum die-casting [J]. *Transactions of Nonferrous Metals Society of China*, 2014, 24: 3769–3776.
- [14] XIAO Lei, YANG Guang-yu, MA Jia-qi, QIN He, LI Jie-hua, JIE Wang-qi. Microstructure evolution and fracture behavior of Mg-9.5Gd-0.9Zn-0.5Zr alloy subjected to different heat treatments [J]. *Materials Characterization*, 2020, 168: 110516.
- [15] LI Jing-long, XIONG Jiang-tao, LI Wen-ya. Physical condition for bonding formation of interfacial atoms in solid-state welding. 10000 selected problems in sciences (manufacturing science) [M]. Beijing: Science Press, 2018: 144–147. (in Chinese)
- [16] GUO Yong-chun, LI Jian-ping, LI Jin-shan, YANG Zhong, ZHAO Juan, XIA Feng, LIANG Min-xian. Mg-Gd-Y system phase diagram calculation and experimental clarification [J]. *Journal of Alloys and Compounds*, 2008, 450(1/2): 446–451.
- [17] JIANG Yong, ZHANG Zuo, GONG Jian-ming. Carbon diffusion and its effect on high temperature creep life of Cr5Mo/A302 dissimilar welded joint [J]. *Acta Metallurgica Sinica*, 2015, 51(4): 393–399.
- [18] WU Yi-ping, ZHANG Xin-ming, DENG Yun-lai, TANG Chang-ping, ZHANG Qian, ZHONG Ying-ying. Microstructure and plastic instability criteria of Mg-Gd-Y-Zr alloy during hot compression [J]. *The Chinese Journal of Nonferrous Metals*, 2014, 24(12): 2961–2968. (in Chinese)
- [19] CZERWINSKI F. The reactive element effect on high-temperature oxidation of magnesium [J]. *International Materials Reviews*, 2015, 60: 264–296.

- [20] ZHANG Kui, LI Xing-gang, LI Yong-jun, MA Ming-long. Effect of Gd content on microstructure and mechanical properties of Mg–Y–RE–Zr alloys [J]. Transactions of Nonferrous Metals Society of China, 2008, 18(S1): s12–s16.
- [21] ZHANG Hao, LI Jing-long, MA Ping-yi, XIONG Jiang-tao, ZHANG Fu-sheng. Effect of grain boundary migration on impact toughness of 316L diffusion bonding joints [J]. Materials Research Express, 2019, 6(7): 076535.
- [22] ZHANG Chao, LI Hong, LI Miao-quan. Role of surface finish on interface grain boundary migration in vacuum diffusion bonding [J]. Vacuum, 2017, 137: 49–55.
- [23] DAS S K, KANG Y B, HA T K, JUNG I H. Thermodynamic modeling and diffusion kinetic experiments of binary Mg–Gd and Mg–Y systems [J]. Acta Materialia, 2014, 71: 164–175.
- [24] CONG Meng-qi, LI Zi-quan, LIU Jin-song, MIAO Xue-fei, WANG Bi-jun, XI Qing-yang. Effect of Gd on microstructure, mechanical properties and wear behavior of as-cast Mg–5Sn alloy [J]. Russian Journal of Non-Ferrous Metals, 2016, 57(5): 445–455.

焊接温度和热处理对 Mg–6Gd–3Y 合金 真空扩散焊接头显微组织和力学性能的影响

马平义^{1,2}, 陈旭^{1,2}, 韩兴^{1,2}, 罗志强^{1,2}, 彭赫力^{1,2}

1. 上海航天精密机械研究所, 上海 201600;

2. 上海金属材料近净成形工程技术研究中心, 上海 201600

摘 要: 在焊接压力 6 MPa、保温时间 90 min、不同焊接温度(400–480 °C)下对 Mg–6Gd–3Y 铸态镁合金进行真空扩散焊试验, 对焊后接头进行(495 °C, 14 h)固溶和(200 °C, 30 h)时效处理, 对接头显微组织和力学性能进行分析。结果表明: 稀土元素及其化合物聚集在焊接界面上, 阻碍晶界向焊接界面另一侧迁移。由于晶粒粗化和固溶强化的综合影响, 焊接态和热处理态接头的抗拉强度均随初始焊接温度增加呈现先增后降的趋势。除焊接温度 400 °C 处理后的接头外, 其他焊接态及固溶处理态的接头均断于母材, 而所有接头经固溶时效处理后均断于焊接界面。焊接温度为 440 °C 时的接头经固溶时效处理后的抗拉强度最高(279 MPa), 此时断后伸长率为 2.8%。

关键词: Mg–Gd–Y 合金; 真空扩散焊; 焊后热处理; 焊接界面; 焊接强度

(Edited by Xiang-qun LI)